could also account for the shift in position of the C-band maximum. The subsidiary maximum (curve 1, Fig. 6) at 220 mμ indicates that some C-band absorption due to point defects is also present.

The two additional bands observed in this work, i.e., a subsidiary maximum at 200 mμ and the 230 mμ band noted after extensive x-ray irradiation and after neutron irradiation, have been examined in detail by the Oak Ridge investigators[7,9,10] by electron spin-resonance and optical-absorption measurements. In a recent paper by Weeks,[11] specific models were suggested for these two defects. The 200-mμ absorption was ascribed to an oxygen divacancy with a trapped electron. The 230-mμ absorption was suggested to be due to an Si-O divacancy with an electron trapped in the defect Si from which the oxygen ion is missing. The results of the present paper do not add to nor do they contradict these models.

ACKNOWLEDGMENT

The expert assistance of James F. Hudson in all phases of this work is gratefully acknowledged.

PHYSICAL REVIEW VOLUME 139, NUMBER 4A 16 AUGUST 1965

Selection Rules for Second-Order Infrared and Raman Processes in the Rocksalt Structure and Interpretation of the Raman Spectra of NaCl, KBr, and NaI

E. BURSTEIN*
Physics Department and Laboratory for Research on the Structure of Matter, University of Pennsylvania, Philadelphia, Pennsylvania

AND

F. A. JOHNSON AND R. LOUDON
Royal Radar Establishment, Malvern, Worchester, England

(Received 15 January 1965)

Group-theoretical selection rules are given for two-phonon infrared absorption and Raman scattering processes in crystals having the rocksalt structure. In common with the diamond structure, two-phonon overtones are infrared inactive. The selection rules for second-order infrared absorption processes in the rocksalt structure are much less favorable than those in the diamond and zinc-blende structures. The selection rules for second-order Raman scattering processes are less restrictive and there are many more Raman-active phonon pairs than infrared-active pairs. With the help of the selection rules, the second-order Raman spectra of NaCl, KBr, and NaI are interpreted in terms of phonon pairs at specific symmetry points in the Brillouin zone, using the theoretical phonon dispersion curves calculated by Hardy and Karo for NaCl and the experimental phonon dispersion curves determined by Woods, Brockhouse, Cowley, and Cochran by neutron spectroscopy for KBr and NaI.

1. INTRODUCTION

THE infrared lattice absorption spectrum of a crystal is due to processes where a photon is absorbed and one or more phonons are emitted into the lattice. In the case of semiconductors with either diamond or zinc-blende structures, the absorption spectrum shows a large amount of detailed structure, arising from two-phonon processes. This structure has been successfully interpreted in terms of a few characteristic phonon energies corresponding to peaks in the combined density-of-states curves.[1] In the case of the alkali halides, however, the infrared lattice absorption bands due to two-phonon emission are relatively few in number and, consequently, precise interpretation is difficult. There are two reasons for this. Firstly, the width of the restrahlen (reflection) band is very much greater in alkali halides than in zinc-blende semiconductors (there is no restrahlen band in diamond-type semiconductors) and masks a number of the expected two-phonon lattice bands. Secondly, as will be shown in Sec. 2, the selection rules for dipole processes in the rocksalt-structure alkali halides are much less favorable than those in the diamond and zinc-blende semiconductors.

The second-order Raman spectrum, which is due to the inelastic scattering of a photon by two phonons, also exhibits structure arising from structure in the combined density-of-states curve.[2] In the case of rocksalt-structure alkali halides the second-order Raman spectra show a wealth of detailed structure. This is primarily due, as will be shown in Sec. 2, to very favorable selection rules for the second-order Raman process. The main purpose of this paper is to show that the peaks in the Raman

* Supported in part by the U. S. Army Research Office-Durham.
[1] F. A. Johnson, *Progress in Semiconductors 9* (Heywood and Company Ltd., London, to be published).
[2] F. A. Johnson and R. Loudon, Proc. Roy. Soc. (London) **A281**, 274 (1964).

spectra of alkali halides can be accounted for by combinations of phonon frequencies at critical points in the Brillouin zone. In the case of NaCl, the analysis of the structure in the Raman spectrum was carried out using the theoretical phonon dispersion of Hardy and Karo[3,4] as a guide for the assignment of phonon frequencies. For KBr and NaI, the assignment of phonon frequencies is based on the neutron-scattering (phonon-dispersion) data of Woods, Brockhouse, Cowley, and Cochran.[5]

2. PHONON SYMMETRIES AND SELECTION RULES

The rocksalt structure has one atom of each kind in the (rhombohedral) unit cell. The two sublattices formed by the two types of atom have face-centered cubic symmetry, and the crystal as a whole has the same symmetry group as the face-centered cubic lattice. The character tables for the symmetry points and lines in the face-centered cubic Brillouin zone have been calculated by Bouckaert, Smoluchowski, and Wigner,[6] and we adhere to the notation of these authors. For any wave vector in the Brillouin zone there are six vibrational modes, whose symmetry characters can be determined by the usual method of placing displacement vectors on the two atoms in the unit cell and examining the transformation properties of their six components under the operations of the appropriate group. The symmetry characters calculated in this way are listed in Table I for all points and lines of symmetry in the zone.

TABLE I. Phonon symmetries in the rocksalt structure.

Symmetry point	Phonon species
Γ	$\Gamma_{15}(0)+\Gamma_{15}(A)$
X	$X_4'(\mathrm{LO})+X_5'(\mathrm{TO})+X_4'(\mathrm{LA})+X_5'(\mathrm{TA})$
L	$L_2'(\mathrm{LO})+L_3'(\mathrm{TO})+L_1(\mathrm{LA})+L_3(\mathrm{TA})$
W	$W_1+W_2'+2W_3$
Δ	$\Delta_1(\mathrm{LO})+\Delta_5(\mathrm{TO})+\Delta_1(\mathrm{LA})+\Delta_5(\mathrm{TA})$
Λ	$\Lambda_1(\mathrm{LO})+\Lambda_3(\mathrm{TO})+\Lambda_1(\mathrm{LA})+\Lambda_3(\mathrm{TA})$
Σ	$2\Sigma_1+2\Sigma_3+2\Sigma_4$
Z	$2Z_1+2Z_3+2Z_4$
Q	$3Q_1+3Q_2$

On the line Q, for which Ref. 6 gives no notation, Q_1 is the identity representation and Q_2 is odd with respect to the single rotation contained in the group. A striking feature of the calculated symmetry characters is the fact that all the phonons at the points Γ and X have negative parity. This is to be contrasted with the corresponding results for the diamond lattice[2] where the optic phonons at Γ have positive parity and parity is undefined for the phonons at X.

The calculation of phonon symmetries gives no indication of the order in which the derived characters are to be assigned to the various phonon branches at a particular symmetry point. At Γ, X, Δ, and Λ, where the vibrations have simple longitudinal or transverse polarization and can be labeled optic or acoustic in an unambiguous way, the assignment of characters to phonon branches is obvious, since corresponding optic and acoustic branches have the same characters and the degeneracy of a branch is sufficient to determine the choice of character. At L, however, corresponding optic and acoustic branches have different symmetries and the assignment has been determined by inspection of unpublished vibrational eigenfunctions derived by Hardy and Karo in their calculations of the phonon spectra of all the rocksalt-structure alkali halides.[3,4] The results of these assignments are indicated in Table I. For the remaining points and lines, the phonon polarizations are not simple. At W, the calculations of Hardy and Karo show that, in order of decreasing frequency, the phonon symmetries are W_3, W_2', W_1, W_3 for NaCl, KBr, and NaI. At small wave vectors close to Γ, the threefold degeneracy of the Γ_{15} optic mode is lifted by electrostatic forces in the usual way to form a twofold degenerate transverse mode and a nondegenerate longitudinal mode.

The selection rules for two-phonon processes in rocksalt can be derived by any of the available group-theoretical methods. Much attention has been given in recent years to the problem of selection-rule determination for processes in perfect crystals where the symmetry of the physical system is governed by a space group. Although the principles of the calculation are the same as apply in the case of selection rules for a system having point-group symmetry, the actual mathematics of the computation of selection rules for space-group symmetry is more involved, owing to the much higher dimensionality of the irreducible representations. This led Elliott and Loudon[7] and Lax and Hopfield[8] to develop simpler methods of calculation using subgroups of the full space-group symmetry. More recently, Birman[9,10] has used the full space group of the diamond lattice to obtain selection rules for two-phonon processes, and Johnson and Loudon[2] have shown that the simpler subgroup method of Ref. 7 leads to identical results. Indeed, Lax[11] has proved that the three methods of selection-rule calculation mentioned above are equivalent. In the present work we have calculated the two-phonon selection rules using the methods of Birman[10] and Elliott and Loudon[7] to provide cross checks on the

[3] J. R. Hardy and A. M. Karo, Phil. Mag. **5**, 859 (1960).
[4] A. M. Karo and J. R. Hardy, Phys. Rev. **129**, 2024 (1963).
[5] A. D. B. Woods, B. N. Brockhouse, R. A. Cowley, and W. Cochran, Phys. Rev. **131**, 1025 (1963).
[6] L. P. Bouckaert, R. Smoluchowski, and E. Wigner, Phys. Rev. **50**, 58 (1936).
[7] R. J. Elliott and R. Loudon, J. Phys. Chem. Solids **15**, 146 (1960).
[8] M. Lax and J. J. Hopfield, Phys. Rev. **124**, 115 (1961).
[9] J. L. Birman, Phys. Rev. **131**, 1489 (1963).
[10] J. Birman, Phys. Rev. **127**, 1093 (1962).
[11] M. Lax, Phys. Rev. **138**, A793 (1965).

TABLE II. Infrared-active two-phonon combinations.

Symmetry point	Active combinations
Γ	None
X	None
L	TO+LA, TO+TA, LO+LA, LO+TA
W	W_1+W_2', W_1+W_3, $W_2'+W_3$
Δ	
Λ	All combinations
Q	
Σ	All combinations except $\Sigma_3+\Sigma_4$
Z	All combinations except Z_3+Z_4

results, which are given in Tables II and III. The former table lists phonon pairs which are active in electric-dipole absorption of infrared radiation, and the latter lists the pairs which are active in the second-order Raman effect. The second-order Raman selection rules at L have previously been given by Born and Bradburn.[12]

The most striking selection rule is that which excludes infrared activity in all two-phonon overtones. This selection rule has previously been derived for the rocksalt lattice by Szigeti,[13] and it can be proved for any crystal lattice which possesses inversion symmetry.[11,14] The selection rules (Tables II and III) show that in rocksalt, as in diamond, there are many more Raman-active phonon pairs than infrared-active pairs. This is particularly striking at the points Γ and X where all phonon pairs are Raman active but none are infrared active. This feature of the selection rules largely explains the lack of structure in the infrared absorption spectra of the alkali halides compared with the relatively abundant structure in their Raman spectra. The underlying reason for the severe infrared selection rules is the presence of inversion symmetry about both atoms in the rocksalt unit cell. This is to be contrasted with the case of zinc blende where the lattice has no inversion symmetry and the infrared selection rules are relatively lenient.[9]

TABLE III. Raman-active two-phonon overtones and combinations.

Symmetry point	Depolarization factor[a]	Active overtones and combinations
Γ	Finite	20
X; Δ	Zero	2LO, 2LA, LO+LA
	Finite	All other overtones and combinations
L	Finite	2LO, 2TO, 2LA, 2TA, LO+TO, LA+TA
W	Zero	W_1+W_2', $2W_1$, $2W_2'$
	Finite	All other overtones and combinations
Λ, Q	Finite	All overtones and combinations
Σ	Zero	$\Sigma_1+\Sigma_4$
	Finite	All overtones and all other combinations
Z	Zero	All overtones
	Finite	All combinations

[a] For incident radiation along the [100] direction and scattered radiation along the [010] direction.

As discussed by Birman[9] and Johnson and Loudon[2] the selection-rule calculation also gives some information about the state of polarization of the scattered radiation in the second-order Raman effect. The polarization of the scattered radiation can be described in terms of the depolarization factor ρ, which is defined as the ratio of the intensity of the component of scattered radiation parallel to the plane of scattering to that of the component perpendicular to the scattering plane. The depolarization factor will depend on the polarization of the incident radiation (i.e., either polarized parallel or perpendicular to the plane of scattering, or unpolarized), on the orientation of the crystal relative to the directions of the incident and scattered radiation, and on the symmetry of the phonons which take part in the scattering.[15] ρ is generally measured for the case where the incident and scattered radiation directions are at right angles to one another.

In first-order Raman scattering, with the incident light unpolarized and directed along [100] and the scattered light observed along [010], Γ_1 and Γ_{12} symmetry phonons yield $\rho=0$ while a Γ_{25}' phonon gives $\rho=2$.[15,16] A phonon of Γ_{15}' symmetry can also give rise to Raman scattering, but the scattered intensity depends on the antisymmetric part of the scattering tensor which is generally one or more orders of magnitude smaller than the symmetric part and can readily be neglected.[17] In second-order scattering, the pair of phonons which participates in the scattering process yields a representation whose reduction contains a sum of irreducible representations.[10] If the sum contains Γ_1 and/or Γ_{12}, but not Γ_{25}' then the two-phonon state is Raman active, and the depolarization factor ρ is zero; if the sum contains Γ_{25}' the state is Raman active with ρ nonzero. The scattering by a specific pair of phonons can thus be characterized by a "zero" or a "finite" depolarization factor. The depolarization character of second-order scattering by particular phonon pairs for incident radiation along [100] and scattered radiation along [010] has been tabulated for diamond structures by Johnson and Loudon.[2] The corresponding depolarization-character results for rocksalt structures are given in Table III. The depolarization character given by Birman[9] for diamond and zinc-blende structures corresponds to an average over-all orientation, as in the molecular case, and is therefore more appropriate for the case of second-order Raman scattering by powdered crystals.

[12] M. Born and M. Bradburn, Proc. Roy. Soc. (London) **A188**, 161 (1947).
[13] B. Szigeti, Proc. Roy. Soc. (London) **A252**, 217 (1959).
[14] R. Loudon, Phys. Rev. **137**, A1784 (1965).
[15] L. Couture and J. P. Mathieu, Ann. Phys. (Paris) **3**, 521 (1948).
[16] B. D. Saksena, Proc. Indian Acad. Sci. **A11**, 229 (1940).
[17] R. Loudon, Proc. Roy. Soc. (London) **A275**, 218 (1963).

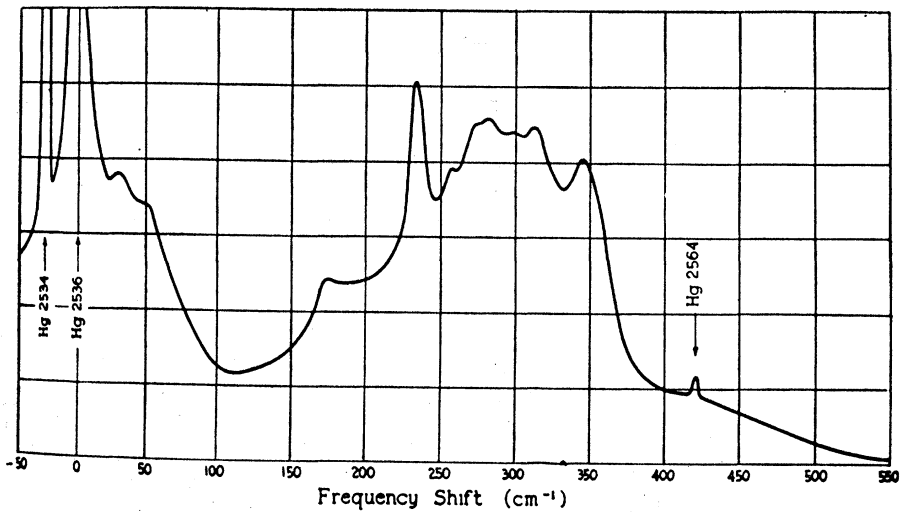

FIG. 1. Room-temperature Raman spectrum of NaCl [H. L. Welsh, M. F. Crawford, and W. J. Staple, Nature 164, 737 (1949)].

3. INTERPRETATION OF OBSERVED RAMAN SPECTRA

1. NaCl

The Raman spectrum of NaCl was first measured in 1931 by Rasetti,[18] and discussed by Fermi and Rasetti[19] who were the first to suggest that the relatively weak scattering spectrum was due to second-order processes. The measurements were repeated by Krishnan[20] in 1945 using higher resolution. The first complete theory of the second-order Raman effect in rocksalt structures was given by Born and Bradburn[12] in 1947 and applied to NaCl using the frequencies of the normal modes calculated by Kellerman[21] on the basis of a rigid-ion model. By assuming that only the displacements of nearest-neighbor atoms contribute to the second-order electronic polarizability and that the major contribution to the combined density of states came from normal modes near the L point, Born and Bradburn were able to account for the main features of the experimental spectrum obtained by Krishnan. Measurements of the Raman spectrum of NaCl at still higher resolution were carried out by Welsh, Crawford, and Staple[22] in 1949. Their spectrum (Fig. 1), which represents the most reliable results for the second-order Raman spectrum of an alkali halide to date, exhibits 11 well-defined peaks (Table IV). The frequency shifts for the nine higher frequency peaks are in good agreement with Krishnan's measurements. However, the two lower frequency peaks do not occur in Krishnan's spectrum, nor is there evidence for the other 10 frequencies which Krishnan reported. For purposes of comparison, the infrared spectrum of NaCl (Fig. 2) exhibits only four well-defined subsidiary peaks.

With the help of the selection rules we have attempted to establish the phonon-pair assignments for the observed peaks in the Raman spectrum of NaCl using the theoretical phonon dispersion curves of Hardy and Karo,[3,4] calculated on the basis of a "deformable dipole" model (Fig. 3). In particular, we used the calculated phonon frequencies at X and L, where critical points occur for all of the phonon branches, and at the points along Δ, where the LO and LA branches have extrema. The phonon assignments which we obtained are given in Table IV. From these phonon assignments

TABLE IV. Second-order Raman peaks in NaCl.

Peak positions in cm^{-1}		
Experimental	Interpretation	Calculated for X point
31	TO−LA(X)	30
55	LA−TA(X) LO−LA(Δ) LA−TA(L)	56
174	2TA(X)	174
234[a]	LA+TA(X) LA+TA(Δ) 2TA(L)	230
256	TO+TA(X) 2TO(L)	260
275	LA+TA(L)	
285	2LA(X)	286
299	LO+TA(X) 2LA(Δ)	299
314	TO+LA(X) 2LA(L)	316
346	2TO(X) LO+LA(Δ) LO+TO(L)	346
415 (broad)	2LO(X) (among others)	414

[a] Strongest peak.

[18] F. Rasetti, Nature 127, 626 (1931).
[19] E. Fermi and F. Rasetti, Z. Physik 71, 689 (1931).
[20] R. S. Krishnan, Nature 156, 267 (1945).
[21] E. W. Kellerman, Phil. Trans. Roy. Soc. (London) A238, 513 (1940).
[22] H. L. Welsh, M. F. Crawford, and W. J. Staple, Nature 164, 737 (1949).

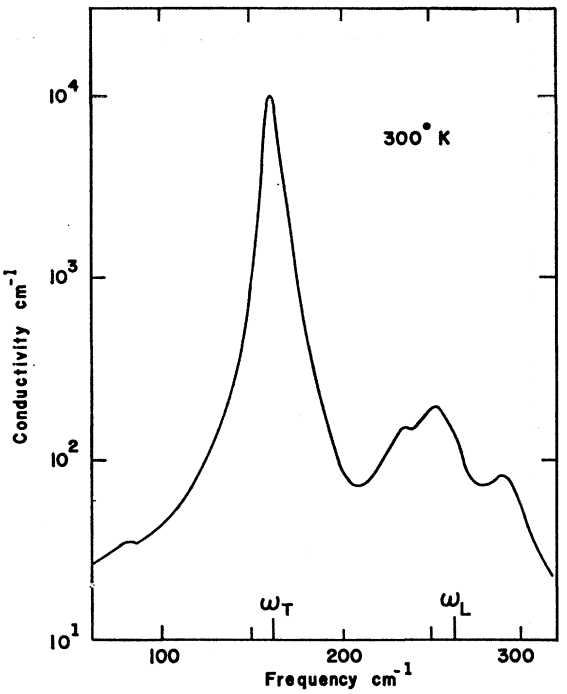

FIG. 2. Room-temperature infrared absorption spectrum of NaCl [after C. Smart, G. R. Wilkinson, A. M. Karo, and J. R. Hardy, *Proceedings of the International Conference on Lattice Dynamics, Copenhagen, 1963* (Pergamon Press, Inc., New York, 1965), p. 383].

and the experimental peak positions we were also able to derive a consistent set of phonon frequencies at the X symmetry point which are within 5% of the phonon frequencies calculated by Hardy and Karo (Table V).

TABLE V. Room-temperature phonon frequencies in NaCl.

Branch	Calculated by Hardy and Karo (Ref. 4) L cm^{-1}	Δ cm^{-1}	X cm^{-1}	Deduced at "X" from Raman effect cm^{-1}
LO	236	196[a]	208	212
TO	123	183	183	173
LA	160	151[a]	140	143
TA	112	75	83	87

[a] The Δ_{LO} and Δ_{LA} branches have extrema at a q/q_{max} of about 0.7.

Using the derived values for the phonon frequencies at X, it is actually possible to account for most of the observed peaks to within 4 cm^{-1} (third column Table IV). This suggests that the peaks in the combined two-phonon density of states in NaCl, making the major contribution to the second-order Raman spectrum, occur at points close to X. Preliminary results of an as yet unpublished calculation of the combined density of states in NaCl by Hardy and Karo show a striking agreement with the observed distribution of intensity in the Raman effect.

2. KBr and NaI

The second-order Raman spectrum of KBr has been measured at room temperature by Menzies and Skinner,[23] Krishnan and Narayanan,[24] Stekhanov and Eliashberg,[25] and most recently, by Raman.[26] The positions of the peaks reported by the various investigators are given in Table VI. In general the positions of peaks reported by two or more investigations are in good agreement with one another. On the other hand, the peaks reported by only a single investigation must for the present be considered as uncertain.

The phonon dispersion curves of KBr have been determined experimentally by Woods, Brockhouse, Cowley, and Cochran using neutron scattering.[5] Detailed measurements were made at 90°K for the [100], [110], and [111] directions. Less extensive measurements were also made at 400°K for the [100] and [111] directions. In deriving the phonon-pair assignments for the observed peaks in the Raman spectrum in terms of the neutron data, we have used values of the phonon frequencies (Table VII) which are intermediate between those measured at 90°K and at 400°K, as approximations for room-temperature values.

Our phonon assignments for the observed peaks and the associated frequencies based on the neutron results are given in the fifth and sixth columns of Table VI. We have not included assignments for peaks reported by a single investigator in view of the uncertainty as to their

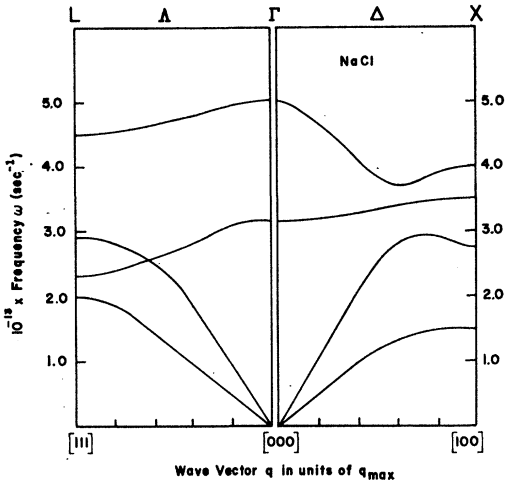

FIG. 3. The frequency-versus-wave-vector curves of NaCl for [100] and [111] directions [after J. R. Hardy and A. M. Karo, Phil. Mag. 5, 859 (1960)].

[23] A. C. Menzies and J. Skinner, J. Phys. Radium **9**, 93 (1948).
[24] R. S. Krishnan and P. S. Narayanan, Proc. Indian Acad. Sci. **A28**, 296 (1948).
[25] A. I. Stekhanov and M. B. Eliashberg, Opt. i Spektroskopiya **10**, 348 (1961) [English transl.: Opt. Spectry. (USSR) **10**, 174 (1961)]; Fiz. Tverd. Tela **2**, 2354 (1960) [English transl.: Soviet Phys.—Solid State **2**, 2096 (1961)].
[26] C. V. Raman, Proc. Indian Acad. Sci. **A57**, 1 (1963).

TABLE VI. Second-order Raman peaks on KBr.

Peak positions in cm^{-1}					
Menzies and Skinner (Ref. 19)	Krishnan and Narayanan (Ref. 20)	Stekhanov and Eliashberg (Ref. 21)	Raman (Ref. 22)	Interpretation	Neutron (Ref. 5)
...	46	44	...	TO−LA(X)[b]	48
				LO−TO(L)	44
...	...	(59)	...		
...	84	83	85	2TA(X)	82
...	...	(90)	...		
...	105	104	...		
127[a]	126[a]	126[a]	122[a]	TA+LA(X)	122
142	146	143	142	2LA(X)	144
				2TA(L)	142
166	170	168	169	LA+TA(L)	164
				TO+TA(L)	169
				LO+TA(X)	174
...	186	187	184	2LA(L)	186
...	...	...	(196)		
212	216	217	215	TA+LO(L)	213
				LO+LA(Δ)	209
...	(230)	...	...		
240	242	...	242	2TO(X)	240
				LO+TO(L)	240
				LO+TO(Δ)	239
...	(287)	...	...		

[a] Strongest peak.
[b] An TO+LA(X) peak should occur at 192 cm^{-1}.

reality. It is seen that the majority of the peaks can be accounted for to within 4 cm^{-1} by the neutron results and that different Raman measurements disagree among themselves by amounts of the same order.

The second-order Raman spectrum of NaI has recently been measured at room temperature by Krishnan and Krishnamurthy.[27] The positions of the prominent peaks are listed in Table VIII. In addition to the peaks listed, the spectrum also exhibits two broad bands in the region of 200–250 cm^{-1} and 310–370 cm^{-1} in which any structure that may be present is apparently masked by "noise." The phonon dispersion curves of NaI at 100°K have also been determined by Woods, Brockhouse, Cowley, and Cochran. Since it was desirable to have room-temperature values of the phonon frequencies in deriving the phonon-pair assignments for the observed peaks, we have used Karo and Hardy's theoretical values of the phonon frequencies at 0°K and at room temperature to estimate the change in frequency on going from 100°K to room temperature (Table IX). Our assignments for the observed peaks and the associated frequencies based on the neutron data extrapolated to room temperature are given in Table VIII.

Cowley[28] has recently carried out a detailed calcula-

TABLE VII. Room-temperature phonon frequencies in KBr from neutron scattering (Ref. 5).

Branch	L cm^{-1}	Δ cm^{-1}	X cm^{-1}
LO	142	122[a]	133
TO	98	~117	120
LA	93	87[b]	72
TA	71	~35	41

[a] Δ_{LO} branch has minimum at a q/q_{max} of about 0.7.
[b] Δ_{LA} branch has maximum at a q/q_{max} of about 0.6.

TABLE VIII. Second-order Raman peaks in NaI.

Peak positions in cm^{-1}		
Experiment (Ref. 23)	Interpretation	Neutron (Ref. 5)
19	LA−TA(X)	21
42	...	...
58	LO−LA(Δ)	62
88	LO−TA(X)[b]	88
103[a]	LA+TA(X)	103
	2TA(L)	100
120	2LA(X)	124
	LA+TA(L)	125
132	2LA(Δ)	136
200	LO+LA(Δ)	198

[a] Strongest peak.
[b] An LO+TA(X) combination should occur at 170 cm^{-1} but may be masked by the presence of the mercury line at 186 cm^{-1}.

[27] R. S. Krishnan and N. Krishnamurthy, Z. Physik **175**, 440 (1963).

[28] R. A. Cowley, Proc. Phys. Soc. (London) **84**, 281 (1964).

TABLE IX. "Room-temperature" phonon frequencies in NaI.[a]

Branch	L cm^{-1}	Δ cm^{-1}	X cm^{-1}
LO	167	130	129
TO	110	120	122
LA	75	68[b]	62
TA	50	36	41

[a] 100°K neutron results (Ref. 5) extrapolated to room temperature using Karo and Hardy's calculated frequency changes with temperature.
[b] Δ_{LA} branch has maximum at a q/q_{max} of about 0.6.

tion of the second-order Raman spectra of KBr and NaI using the shell model to obtain expressions for the dependence of the electronic polarizability on the normal modes of vibration, and using the frequencies and eigenvectors of the normal modes calculated by Cowley, Cochran, Woods, and Brockhouse[29] to obtain the combined density of states. Cowley's results for the frequency of the peaks, which depend slightly on the orientation of the crystal, are in good agreement with the experimental values. However, the strongest peaks in the calculated spectra, at 247 cm^{-1} for KBr and at 242 cm^{-1} for NaI correspond to rather weak peaks in the observed spectra. Since these peaks arise from combinations and overtones of longitudinal-optic (LO) and/or transverse-optic (TO) phonons, it appears that Cowley's calculations lead to an appreciable overestimate of the matrix elements for these phonons.

3. Polarization Effects

The polarization of the second-order scattered radiation has been investigated for a number of rocksalt-structure alkali halides. Menzies and Skinner[23,30] have obtained qualitative information about the depolarization factors of the peaks in the Raman spectra of NaCl, NaBr, KCl, KBr, and RbBr. They observed that for NaCl, NaBr, and KBr the "major peak" in the spectrum was "depolarized" with $\rho \geq 1$ and the rest of the spectrum was "polarized" with $\rho < 1$, whereas for KCl and RbBr there was no outstanding peak and the spectrum was weaker and everywhere "polarized." (In KI, studied by Krishnan and Narayanan[31] and by Stekhanov and Petrova,[32] the "major peak" was also found to be "depolarized" while the rest of the spectrum was "polarized.") Since the cation-to-anion mass ratio is close to unity in KCl and RbBr and is appreciably less than unity in NaCl, NaBr, and KBr, Menzies and Skinner[23] have suggested that the difference in behavior of the two groups of crystals may be associated with the differences in the cation-to-anion mass ratios and their effects on the shape of the phonon dispersion curves.

In his calculations of the second-order Raman spectra of KBr and NaI, Cowley finds that the intensities and the depolarization factors of the peaks are strongly dependent on the orientation of the crystal specimen. Since Menzies and Skinner do not state the orientation of the specimens used in their polarization studies, Cowley was not able to compare their results with his theoretical calculations.

According to our phonon-pair assignments for the observed peaks in the Raman spectra of NaCl, KBr, and NaI, the "major peaks" in NaCl and NaI arise from an LA+TA(X or Δ) combination, and or a 2TA(L) overtone, and the "major peak" in KBr arises from an LA+TA(X or Δ) combination. Since an LA+TA(X or Δ) combination peak and a 2TA(L) overtone peak are associated with finite depolarization factors (Table III), our assignments for the "major peaks" are, at least, consistent with the observed polarization results. It is of interest to note that a preliminary analysis of the Raman spectra of NaBr and KI based on Karo and Hardy's theoretical phonon dispersion curves[4] indicates that the LA+TA(X or Δ) and 2TA(L) assignments are also applicable to the "major peaks" in these crystals.

4. CONCLUSION

We have demonstrated in the case of NaCl how the observed structure in the Raman spectrum can be interpreted, with the help of the theoretical phonon dispersion curves of Hardy and Karo,[3] in terms of phonon pairs at specific symmetry points in the Brillouin zone corresponding to density-of-states maxima. Our results indicate that the phonons at (or near) the X point play a major role in the scattering. Although the experimental data are less satisfactory for KBr and NaI, we have shown that much of the observed structure can be directly correlated with the known neutron data for these two materials.

We would expect that accurate and detailed measurements of the Raman spectrum made with the highest resolution would show slope discontinuities characteristic of critical points in the phonon spectrum.[2] Depolarization measurements for several orientations of the crystal would be particularly useful in distinguishing between certain critical points. The use of laser sources and more refined photometric techniques may be expected to provide this type of information in the near future. These, together with measurements over a wide temperature range, would enable one to make a more detailed analysis and should result in precise values for the energies of the phonons at symmetry points.

ACKNOWLEDGMENTS

The authors wish to thank Dr. J. R. Hardy and Dr. A. M. Karo for helpful discussions, and for allowing them to use unpublished tables of their calculations. They also wish to thank Dr. S. Ganesan for valuable discussions and Professor R. S. Krishnan for communicating his NaI Raman spectrum in advance of publication.

[29] R. A. Cowley, W. Cochran, A. D. B. Woods, and B. N. Brockhouse, Phys. Rev. **131**, 1030 (1963).
[30] A. C. Menzies and J. Skinner, J. Chem. Phys. **46**, 60 (1949).
[31] R. S. Krishnan and P. S. Narayanan, J. Indian Inst. Sci. **39**, 85 (1957).
[32] A. I. Stekhanov and M. L. Petrova, Zh. Eksperim. i Teor. Fiz. **19**, 1108 (1949).